J|A|C|S COMMUNICATIONS

Published on Web 10/27/2009

Evidence of Significant Covalent Bonding in $Au(CN)_2^-$

Xue-Bin Wang,[†] Yi-Lei Wang,[‡] Jie Yang,[†] Xiao-Peng Xing,[†] Jun Li,*[,‡] and Lai-Sheng Wang*[,§]

Department of Physics, Washington State University, 2710 University Drive, Richland, Washington 99354, Chemical & Materials Sciences Division, Pacific Northwest National Laboratory, MS K8-88, P.O. Box 999, Richland, Washington 99352, Department of Chemistry and Key Laboratory of Organic Optoelectronics and Molecular Engineering of the Ministry of Education, Tsinghua University, Beijing 100084, China, and Department of Chemistry, Brown University, Providence, Rhode Island 02912

Received September 23, 2009; E-mail: junli@tsinghua.edu.cn; lai-sheng_wang@brown.edu

Recently there has been intense interest in the homogeneous catalytic chemistry of Au(I) complexes.[1] Among the Au(I) molecules, the $Au(CN)_2^-$ ion is the most stable and has been widely used in gold extraction back to ancient times. Although AuCN in the condensed phase has been studied via both solution-phase vibrational spectroscopy[2] and crystal structures,[3] the free AuCN molecule has been studied only very recently by microwave spectroscopy.[4] The important $Au(CN)_2^-$ complex has not been observed and studied in the gas phase. Because of relativistic effects,[5] Au-containing molecules exhibit distinctly different properties among the coinage elements. To elucidate the nature of the Au−ligand binding, high-level ab initio calculations are needed because of the complicated electron correlation and relativistic effects.[6−8] The structure and bonding of the AuCN molecule were first examined computationally by Frenking and co-workers.[7] Recent high-precision calculations by Pyykkö and co-workers[8] suggested multiple-bond character in the Au−C bonds in AuCN because the Au−C bond length is only slightly longer than the sum of the triple-bond covalent radii.

Photoelectron spectroscopy (PES) combined with high-level ab initio calculations is a powerful method for probing the electronic and structural properties of metal complexes without the complication of condensed-phase environments.[9] Our previous PES studies of the Au−halogen complexes AuX_2^- (X = Cl, Br, and I)[10] have stimulated several theoretical calculations,[11] and the well-resolved spectra have served as benchmarks for calibrating theoretical methods for Au-containing systems. A recent PES and high-level ab initio study of AuO^- and AuS^- revealed surprising covalent bonding character in these simple diatomic systems.[12] To probe the nature of the chemical bonding in $Au(CN)_2^-$, here we performed a joint PES and theoretical [including ab initio and density functional theory (DFT) methods] study of the three coinage-metal cyanide complexes $M(CN)_2^-$ (M = Cu, Ag, Au). We obtained PES spectra of $Au(CN)_2^-$ at three detachment photon energies, 6.424 eV (193 nm), 7.866 eV (157 nm), and 10.488 eV (118 nm), and compared them with those of its lighter congeners, $Cu(CN)_2^-$ and $Ag(CN)_2^-$, at 193 and 157 nm. The PES spectra of $Au(CN)_2^-$ display well-resolved vibrational progressions due to the Au−C stretching, in sharp contrast to the atomic-like transitions observed for the mainly ionic $Cu(CN)_2^-$ complex, and thus provide direct experimental evidence of significant covalent bonding character in $Au(CN)_2^-$. Theoretical calculations were carried out to provide insight into the nature of the chemical bonding in $Au(CN)_2^-$ in comparison with that in $Cu(CN)_2^-$ and $Ag(CN)_2^-$.

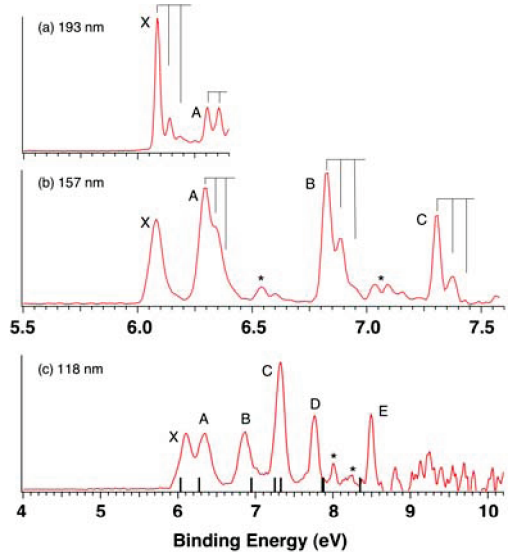

Figure 1. Photoelectron spectra of $Au(CN)_2^-$ at (a) 193 and (b) 157 at 12 K and (c) at 118 nm at room temperature. Resolved vibrational features in the 12 K spectra are labeled. The short bars in (c) represent the positions of theoretical vertical detachment transitions. Features marked with * are likely due to multielectron processes.

The $M(CN)_2^-$ (M = Cu, Ag, Au) complexes were produced via electrospray of 10^{-4} M water/methanol solutions of the respective potassium salts. All of the 193 and 157 nm PES spectra were obtained using our low-temperature PES apparatus operated at 12 K,[13] whereas the 118 nm spectrum for $Au(CN)_2^-$ was taken using our room-temperature instrument.[14] The 118 nm photons were generated via tripling of the 355 nm output from a Nd:YAG laser, as described previously,[15] allowing high-binding-energy features beyond 7.8 eV to be probed. Figure 1 presents the PES spectra of $Au(CN)_2^-$ at three photon energies: 193, 157, and 118 nm. Six major detachment bands (labeled as X and A−E) were observed in the energy range from 6 to 8.5 eV (Table 1). A weak broad feature around 9.2 eV was also discernible, but the signal-to-noise ratio in the high-binding-energy region was poor because of strong background electrons at 118 nm. Vibrational progressions were observed for bands X and A at 193 nm (Figure 1a) and for A, B, and C at 157 nm (Figure 1b), with frequencies of 400 cm^{-1} for X and A, 480 cm^{-1} for B, and 520 cm^{-1} for C. The vibrational features should correspond to Au−C stretching according to solution-phase data[6] and our calculated vibrational frequencies. The adiabatic detachment energy (ADE) of $Au(CN)_2^-$ [or the electron affinity of $Au(CN)_2$] was determined from the 0−0 transition of band X to be 6.09 eV (Table 1). The vertical detachment energies (VDEs) for bands X, A, B, and C are the same as the corresponding ADEs

[†] Washington State University and Pacific Northwest National Laboratory.
[‡] Tsinghua University.
[§] Brown University.

10.1021/ja908106e CCC: $40.75

Table 1. Observed and Calculated Vertical Detachment Energies (VDEs) for $M(CN)_2^-$ (M = Au, Ag, Cu), Observed Vibrational Frequencies, and Final State Assignments

			VDE (eV)[a]		
	feature	state	exptl	calcd	vib freq (cm^{-1})[a]
$Au(CN)_2^-$	X	$^2\Sigma_{1/2g}$	6.09(1)[b]	6.02	400(40)
	A	$^2\Pi_{3/2g}$	6.30(1)	6.28	400(40)
	B	$^2\Delta_{5/2g}$	6.83(1)	6.94	480(40)
	C	$^2\Pi_{1/2g}$	7.31(1)	7.24	520(40)
		$^2\Sigma_{1/2u}$		7.32	
	D	$^2\Pi_{3/2u}$	7.76(2)	7.87	
		$^2\Pi_{1/2u}$		7.88	
	E	$^2\Delta_{3/2g}$	8.50(2)	8.35	
$Ag(CN)_2^-$	X	$^2\Sigma_{1/2g}$	6.06(1)[b]	6.07	400(40)
	A	$^2\Pi_{3/2g}$	6.87(2)	6.92	
	B	$^2\Sigma_{1/2u}$	6.96(1)	7.04	
	C	$^2\Pi_{1/2g}$	7.21(1)	7.13	
	D	$^2\Pi_{3/2u}$	7.67(1)	7.71	
		$^2\Pi_{1/2u}$		7.71	
		$^2\Delta_{5/2g}$		8.09	
		$^2\Delta_{3/2g}$		8.51	
$Cu(CN)_2^-$	X	$^2\Sigma_{1/2g}$	5.29(1)[b]	5.22	
	A	$^2\Pi_{3/2g}$	5.80(1)	5.76	
	B	$^2\Pi_{1/2g}$	5.92(1)	5.88	
	C	$^2\Delta_{5/2g}$	~6.15	6.10	
	D	$^2\Delta_{3/2g}$	~6.4	6.29	
	E	$^2\Sigma_u$	7.10(1)	7.07	
	F	$^2\Pi_u$	7.51(1)	7.61	

[a] Each number in parentheses represents the experimental uncertainty in the last digit. [b] Also the adiabatic detachment energy of the $M(CN)_2^-$ anions or electron affinity for neutral $M(CN)_2$.

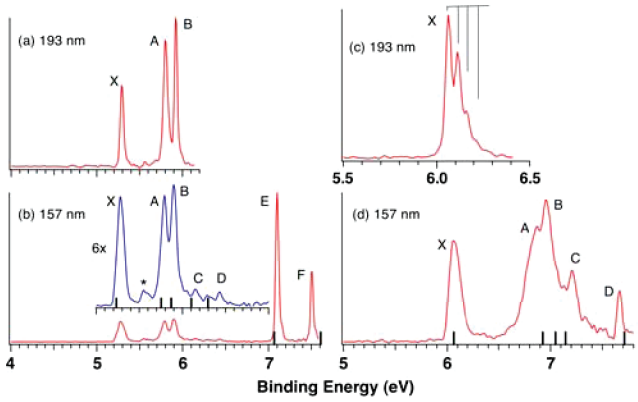

Figure 2. Photoelectron spectra of (a, b) $Cu(CN)_2^-$ and (c, d) $Ag(CN)_2^-$ at 193 and 157 nm at 12 K. The short bars in (b) and (d) represent the calculated vertical detachment energies. The feature marked with * in (b) is likely due to multielectron processes.

because of the short vibrational progressions, whereas the VDEs for bands D and E observed in the 118 nm spectrum (Figure 1c) were measured from the maximum of each band.

The spectrum of $Cu(CN)_2^-$ at 193 nm shows three sharp transitions, designated X, A, and B (Figure 2a). At 157 nm, two strong peaks (E and F) were found at high binding energies (Figure 2b). All of these PES transitions are atomic-like (with the spectral width limited only by the instrumental resolution), in sharp contrast to the vibrationally resolved bands for $Au(CN)_2^-$. Some weak features between the X and A bands (labeled by *) and between B and E (labeled as C and D; see the inset in Figure 2b) were also discernible. The 193 nm spectrum of $Ag(CN)_2^-$ (Figure 2c) exhibits a well-resolved vibrational progression with a spacing of 400 cm^{-1}, most likely due to the Ag−C stretching. The 157 nm spectrum (Figure 2d) shows congested spectral features around 7 eV with three overlapping bands (A, B, and C) and a sharp peak (D) at the high-binding-energy side. The VDEs for all of the observed PES features for $Cu(CN)_2^-$ and $Ag(CN)_2^-$ are also given in Table 1 along with computed values for comparison.

High-level calculations were carried out to optimize structures, compute VDEs, and analyze chemical bonding.[16] The optimized geometries of $M(CN)_2^-$ (M = Cu, Ag, Au) and the corresponding neutrals are all linear (Table S1 in the Supporting Information). The calculated Au−C bond length is 1.99 Å, which lies in the range of experimentally measured Au−C distances in solid $Au(CN)_2^-$ salts (1.98−2.12 Å).[3] The electron binding energies corresponding to one-electron transitions from the closed-shell ground states of the anions to the ground and excited states of the neutrals were obtained using a CASSCF/CCSD(T)/spin−orbit (SO) approach, where the SO splittings were calculated on the basis of CASSCF wave functions with the diagonal matrix elements replaced by the UCCSD(T) energies.[17] The calculated ADEs of $Cu(CN)_2^-$, $Ag(CN)_2^-$, and $Au(CN)_2^-$ were 5.22, 6.03, and 6.02 eV, respectively, in excellent agreement with the experimental data (Table 1). While there is almost no Cu−C bond length change in going from the anion to the neutral (1.89 to 1.88 Å), the Au−C and Ag−C bonds shorten appreciably (1.99 to 1.97 and 2.07 to 2.05 Å, respectively, at the SO PW91 level) (Table S1), consistent with the observed vibrational progressions in the Au−C and Ag−C stretching modes (Figures 1 and 2c). The calculations also predicted electron binding energies for the excited states of the neutrals, which are compared to the spectra as vertical bars in Figures 1 and 2. For $Au(CN)_2^-$ and $Ag(CN)_2^-$, the predicted VDEs agree well with the experimental data, and their assignments are given in Table 1. For $Cu(CN)_2^-$, there is a one-to-one correspondence between the calculated VDEs and the X, A, and B peaks as well as the E and F peaks. However, the calculations also predicted two transitions ($^2\Delta_g$) at 6.10 and 6.29 eV, which lie in between the two major spectral features B and E and are tentatively assigned to the two very weak features C and D (see the Figure 2b inset). However, the relatively small detachment cross sections for C and D were surprising. These two transitions correspond to detachment from the nonbonding δ_g orbitals, and the small detachment cross sections may be correlated with the tightly contracted character of the Cu 3d orbitals. For $Ag(CN)_2^-$, the corresponding detachment channels occur at much higher binding energies (Table 1) and were not observed in the 157 nm spectrum. For $Au(CN)_2^-$, the detachments from the δ_g orbitals have much larger cross sections, occur at a much lower VDE with a large SO splitting, and correspond to the B and E bands, respectively (Table 1). The B band was resolved with a short vibrational progression, suggesting significant covalent bonding character that is very different from the atomic-like nature in $Cu(CN)_2^-$. Features marked with * in Figures 1 and 2 are likely due to multielectron transitions, suggesting strong electron-correlation effects.

The vibrational progressions observed in the spectra of $Au(CN)_2^-$ provide a striking contrast to the atomic-like transitions in the spectra of $Cu(CN)_2^-$. Although the molecular orbital pictures (Figure S1) for the three $M(CN)_2^-$ species look similar, their electronic structures as revealed by the PES data are very different. Table S2 shows that the SO effects in $Au(CN)_2^-$ are much stronger than those in its lighter congeners, which is also reflected in Table S1, where the Au−C bond length in $Au(CN)_2$ shows a sizable reduction upon inclusion of SO effects, resulting in an appreciable Au−C bond length change in going from the anion to the neutral (1.99 to 1.97 Å), in accord with the observed Au−C vibrational progression (Figure 1). The observed vibrational progressions in the photodetachment transitions of $Au(CN)_2^-$ provide direct experimental evidence for covalency in the Au−C bonding. The Au−C bond length (1.99 Å) in $Au(CN)_2^-$ is significantly smaller

Table 2. Theoretical Charge Populations and Bond-Order Analysis for $M(CN)_2^-$ (M = Cu, Ag, Au)[18]

	Charge Population			
M	NPA	Hirshfeld	Voronoi	MDC-q
Cu	0.49	0.14	0.19	0.30
Ag	0.44	0.14	0.20	0.43
Au	0.31	0.04	0.11	0.22
		Bond Order		
M−C	Wiberg		G-J	N-M (3)
Cu−C	0.49		0.51	0.49
Ag−C	0.48		0.50	0.48
Au−C	0.58		0.58	0.57

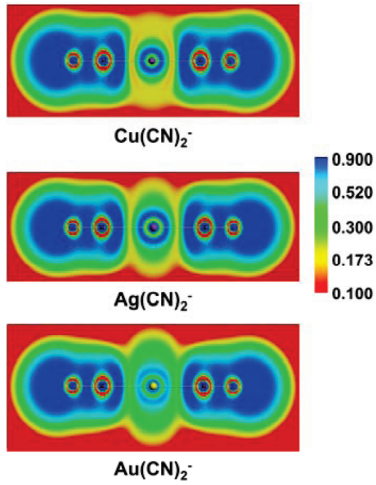

Figure 3. ELFs for $M(CN)_2^-$ (M = Cu, Ag, Au).

than the Ag−C bond length (2.07 Å) in $Ag(CN)_2^-$ and is similar to the Au−C bond length in monoligated AuCN (1.91 Å), which has been suggested to possess triple-bond character.[8] The atomic-like PES transitions in $Cu(CN)_2^-$ are consistent with the ionic bonding nature of this system,[9b] whereas the bonding in $Ag(CN)_2^-$ should be in between.

The nature of the chemical bonding in $M(CN)_2^-$ (M = Cu, Ag, Au) can also be inferred from the population and bond-order analysis results given in Table 2. There is clearly less positive charge on Au and a larger Au−C bond order in $Au(CN)_2^-$ than in the $Cu(CN)_2^-$ and $Ag(CN)_2^-$ complexes. Electron localization functions (ELFs)[19] reflecting the probability to find electron pairs reveal more vividly the increased covalency in the Au−C bonding in $Au(CN)_2^-$, as shown in Figure 3. Fragment orbital analysis and orbital interaction analysis (Table S3) both reveal that the covalent character of Au−C and the remarkable stability of $Au(CN)_2^-$ stem from the strong relativistic effects in gold. The s−d hybridization significantly enhances the ability of Au to form covalent bonds with multiple-bond character. The covalent nature of the Au−C bonding is consistent with the high stability of the $Au(CN)_2^-$ complex.

Acknowledgment. The experimental work carried out in Richland was supported by the U.S. Department of Energy (DOE), Office of Basic Energy Sciences, Division of Chemical Sciences, Geosciences and Biosciences, and by the National Science Foundation (CHE-0749496) and performed at the W. R. Wiley Environmental Molecular Sciences Laboratory, a national scientific user facility sponsored by DOE's Office of Biological and Environmental Research and located at Pacific Northwest National Laboratory, which is operated for DOE by Battelle. The theoretical work was supported by NKBRSF (2006CB932305, 2007CB815200) and NSFC (20525104, 20933003) in China. The calculations were performed using an HP Itanium2 cluster at Tsinghua National Laboratory for Information Science and Technology and at Shanghai Supercomputing Center.

Supporting Information Available: Experimental and theoretical methods; Cartesian coordinates, bond lengths, and stretching vibrational frequencies for $M(CN)_2^-$ (M = Cu, Ag, Au) at the PW91 level of theory; frontier occupied molecular orbitals of $M(CN)_2^-$ (M = Cu, Ag, Au); assignments of the photoelectron spectra and contributions of SO-free states to SO eigenstates; and fragment analysis for $M(CN)_2^-$ (M = Cu, Ag, Au) with the M and CN neutrals as fragments. This material is available free of charge via the Internet at http://pubs.acs.org.

References

(1) Gorin, D. J.; Toste, F. D. *Nature* **2007**, *446*, 395.
(2) (a) Jones, L. H. *J. Chem. Phys.* **1957**, *27*, 468. (b) Chadwick, B. M.; Frankiss, S. G. *J. Mol. Struct.* **1976**, *31*, 1. (c) Willner, H.; Schaebs, J.; Hwang, G.; Mistry, F.; Jones, R.; Trotter, J.; Aubke, F. *J. Am. Chem. Soc.* **1992**, *114*, 8972.
(3) (a) Bowmaker, G. A.; Kennedy, B. J.; Reid, J. C. *Inorg. Chem.* **1998**, *37*, 3968. (b) Hibble, S. J.; Hannon, A. C.; Cheyne, S. M. *Inorg. Chem.* **2003**, *42*, 4724. (c) Rosenzweig, A.; Cromer, D. T. *Acta Crystallogr.* **1959**, *12*, 709. (d) Assefaa, Z.; Kalachnikovab, K.; Hairec, R. G.; Sykora, R. E. *J. Solid State Chem.* **2007**, *180*, 3121.
(4) Okabayashi, T.; Okabayashi, E. Y.; Koto, F.; Ishida, T.; Tanimoto, M. *J. Am. Chem. Soc.* **2009**, *131*, 11712.
(5) Pyykkö, P. *Angew. Chem., Int. Ed.* **2004**, *43*, 4412.
(6) Schwerdtfeger, P.; Boyd, P. D. W.; Burrell, A. K.; Robinson, W. T. *Inorg. Chem.* **1990**, *29*, 3593.
(7) Dietz, O.; Rayn, V. M.; Frenking, G. *Inorg. Chem.* **2003**, *42*, 4977.
(8) Zaleski-Eigierd, P.; Patzschke, M.; Pyykkö, P. *J. Chem. Phys.* **2008**, *128*, 224303.
(9) (a) Waters, T.; Wang, X. B.; Wang, L. S. *Coord. Chem. Rev.* **2007**, *251*, 474. (b) Boldyrev, A. I.; Li, X.; Wang, L. S. *J. Chem. Phys.* **2000**, *112*, 3627.
(10) Schröder, D.; Brown, R.; Schwerdtfeger, P.; Wang, X. B.; Yang, X.; Wang, L. S.; Schwarz, H. *Angew. Chem., Int. Ed.* **2003**, *42*, 311.
(11) (a) Dai, B.; Yang, J. *Chem. Phys. Lett.* **2003**, *379*, 512. (b) Mishra, S. *J. Phys. Chem. A* **2007**, *111*, 9164. (c) Mishra, S.; Vallet, V.; Domcke, W. *ChemPhysChem* **2006**, *7*, 723.
(12) Zhai, H. J.; Bürgel, C.; Bonacic-Koutecky, V.; Wang, L. S. *J. Am. Chem. Soc.* **2008**, *130*, 9156.
(13) Wang, X. B.; Wang, L. S. *Rev. Sci. Instrum.* **2008**, *79*, 073108.
(14) Wang, L. S.; Ding, C. F.; Wang, X. B.; Barlow, S. E. *Rev. Sci. Instrum.* **1999**, *70*, 1957.
(15) Yang, J.; Wang, X. B.; Xing, X. P.; Wang, L. S. *J. Chem. Phys.* **2008**, *128*, 201102.
(16) Geometries were optimized at the DFT PW91/TZ2P level with frozen cores (Cu.3p, Ag.4p, Au.4f, C.1s, N.1s) using ADF 2007.1. SO-free energies were obtained with UCCSD(T) and the SO matrix elements at the CASSCF level using MOLPRO 2008.1. In the UCCSD(T) and CASSCF calculations, effective core potentials with 10, 28, and 60 electrons in the cores for Cu, Ag, and Au, respectively, and aug-cc-pVTZ basis sets were used.
(17) Berning, A.; Schweizer, M.; Werner, H.-J.; Knowles, P. J.; Palmieri, P. *Mol. Phys.* **2000**, *98*, 1823.
(18) See the Supporting Information for detailed theoretical methods.
(19) (a) Becke, A. D.; Edgecombe, K. E. *J. Chem. Phys.* **1990**, *92*, 5397. (b) Savin, A.; Flad, J.; Preuss, H.; Jepsen, O.; Andersen, O. K.; von Schnering, H. G. *Angew. Chem.* **1992**, *104*, 186.

JA908106E